

# Driving the SEPCaster Model with an Automated Solar Active Region Identification and Characterization Module

Sailee M. Sawant<sup>1</sup>, Gang Li<sup>1</sup>, and Meng Jin<sup>2</sup>

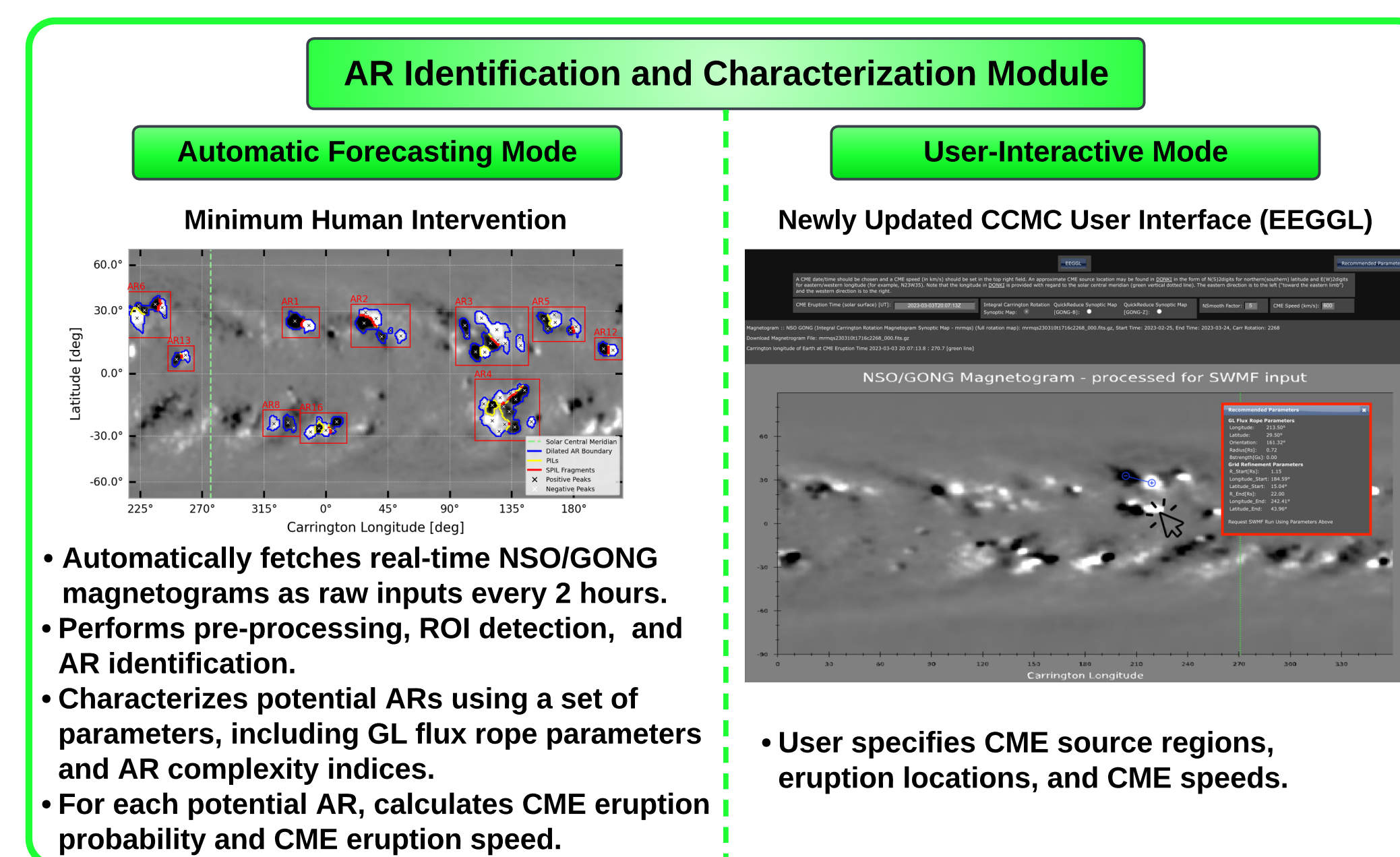
<sup>1</sup>Department of Space Science and CSPAR, University of Alabama in Huntsville, Huntsville, AL 35899, USA

<sup>2</sup>Lockheed Martin Solar and Astrophysics Laboratory, Palo Alto, CA 94304, USA

## SCIENTIFIC BACKGROUND

Solar flares and coronal mass ejections (CMEs) can cause disruptive space weather conditions, including geomagnetic storms and solar energetic particle (SEP) events, which may severely damage ground- and space-based technological systems and affect our daily lives. Therefore, we require state-of-the-art forecasting models to accurately predict space weather phenomena. **This research aims to develop a physics-based operational SEP forecast model, SEPCaster, for the energetic particle radiation environment in the inner Solar System and Earth's magnetosphere.**

## SEPCaster MODEL



This presentation focuses on our new automated Python-based module (shown in green) for identifying and characterizing solar active regions (ARs).

## ROI DETECTION

- Pre-processes the acquired NSO/GONG magnetogram by applying a **Gaussian smoothing** filter with a 5 x 5 kernel. This step suppresses the complexity of the magnetic field configuration<sup>1</sup>.
- Uses `photutils.segmentation`<sup>2</sup>, an affiliated package of AstroPy<sup>3</sup>, to detect positive and negative regions of interest (ROIs) with pixel values greater than pre-defined intensity thresholds (e.g., 1 $\sigma$ , 2 $\sigma$ , and 3 $\sigma$ ). We apply a combination of **multi-thresholding**<sup>2</sup> and **watershed segmentation**<sup>2</sup> techniques to deblend relatively complex ROIs at an intensity threshold of 1 $\sigma$ .
- Computes **flux-weighted centroids** of the detected ROIs.
- Implements **structural thresholding** and removes ROIs smaller than a pre-defined area threshold (e.g., 10 pix<sup>2</sup>).

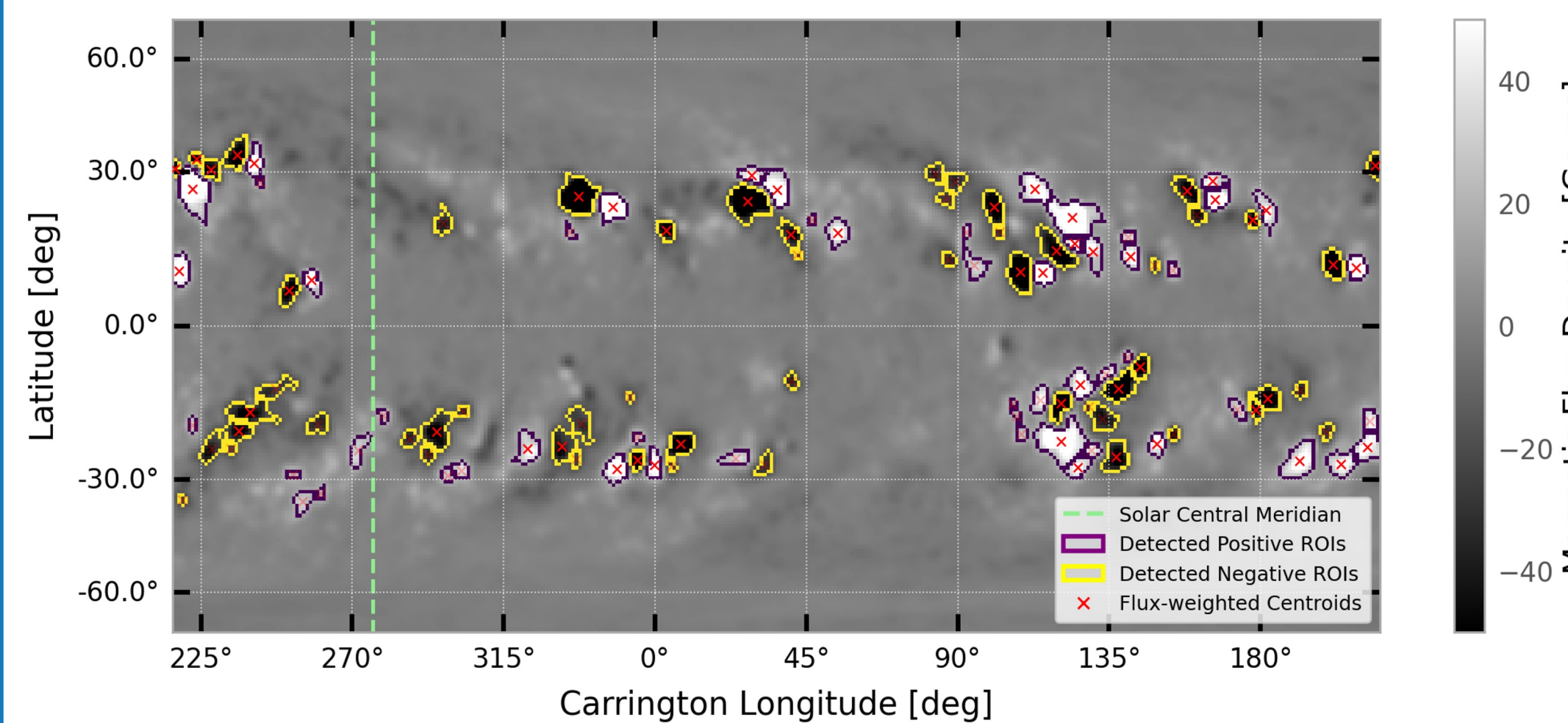


**Figure 1:** Pre-processed NSO/GONG MRBQS magnetogram for Carrington Rotation 2268 obtained on March 03, 2023 at 11:04 UTC. Positive and negative ROIs are detected at an intensity threshold of 1 $\sigma$ .

## AR IDENTIFICATION

- Implements an **agglomerative hierarchical algorithm**<sup>4</sup> to identify potential ARs from the detected ROIs.
  - Validates the total number of clusters using the silhouette score<sup>5</sup>, root-square<sup>6</sup> (RS), and root-mean-square-standard deviation<sup>6</sup> (RMSSTD) indices.
  - Calculates the RMSSTD/RS ratio (i.e., the fraction of intra-cluster distances to inter-cluster distances) to determine the optimal number of clusters.
- Uses physics-informed constraints to refine results:
  - Adds/Removes ROIs to/from the acquired clusters using the **area-distance correlation criterion**.
  - Imposes the **flux-balance mechanism criterion**.
  - Verifies that each cluster contains at least **one ROI of opposite polarity**.

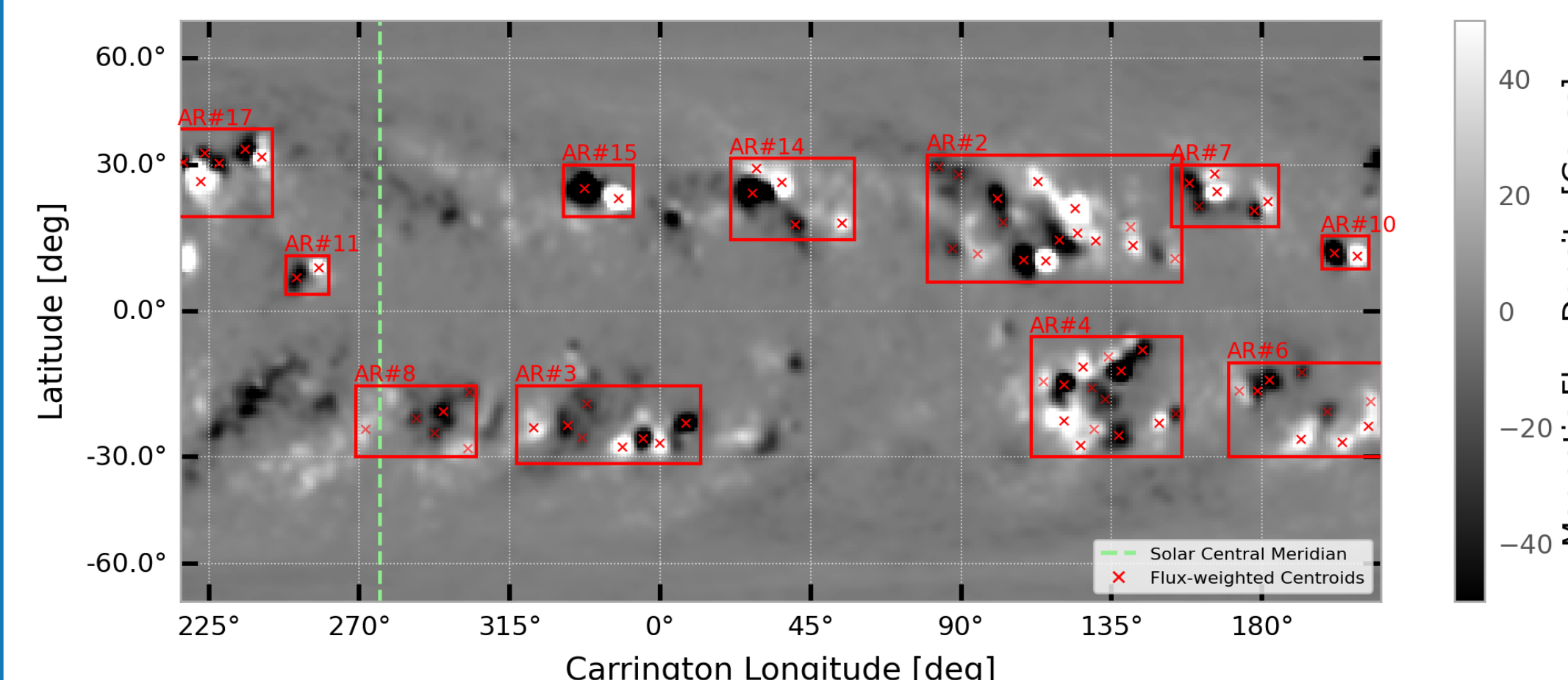


**Figure 2:** Potential ARs (red boxes) for the pre-processed NSO/GONG MRBQS magnetogram shown in Figure 1.

## AR CHARACTERIZATION

- Characterizes the identified potential ARs using **parameters listed in Table 1 of Steward et. al. (2017)**. Some of the important parameters include number of flux peaks, total unsigned flux, total area, number of polarity inversion lines (PILs) and strong-gradient PILs (SPILs), length of PILs and SPILs, and longitudinal and latitudinal gradients.
- Calculates AR complexity indices using our modified version of **correlation dimension mapping**<sup>7</sup> (CDM).

### BOUNDARY- AND AREA-BASED AR COMPLEXITY INDICES

Mason & Uritsky (2022) originally introduced CDM to quantify the irregularities in coronal hole boundaries. We extend the application of CDM to ARs and define our own boundary- and area-based AR complexity indices. This provides an additional way to characterize the identified ARs and helps in determining their potential for eruptive activity.

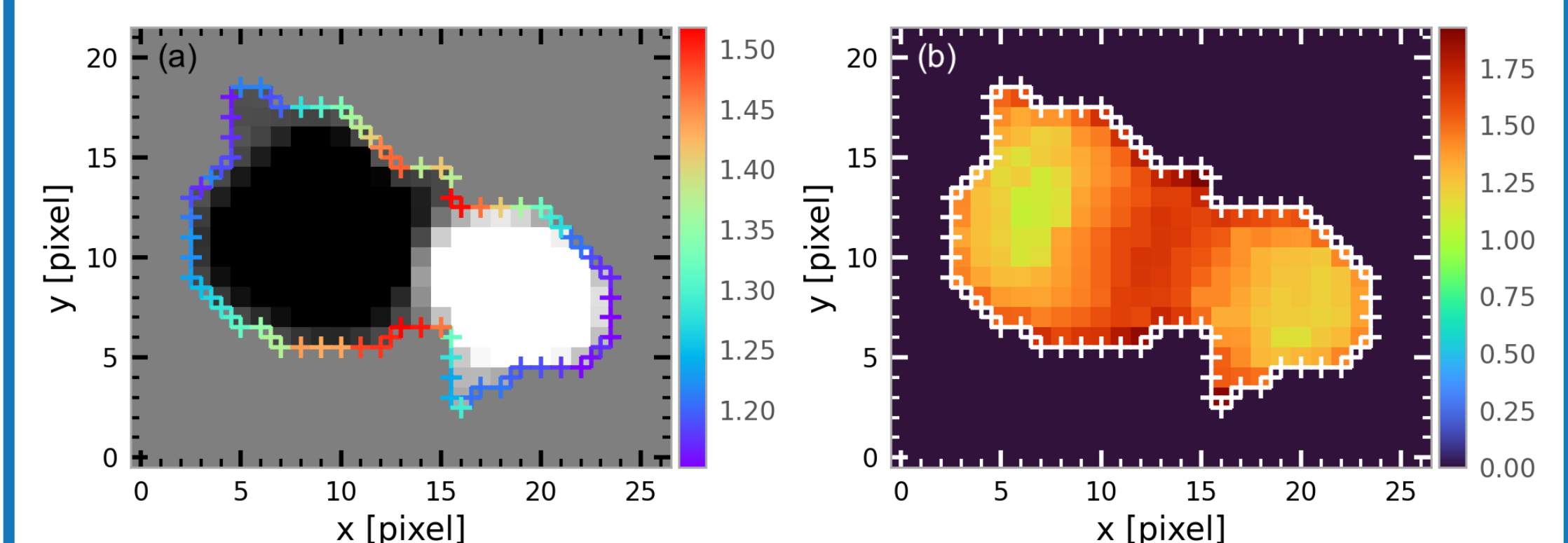


**Figure 3:** Examples of (a) boundary- and (b) area-based CDMs for AR1 identified in Figure 2. The boundary- and area-based CDM indices for AR1 are 1.301 and 1.435, respectively.

## POTENTIAL CME ERUPTION SPEED

Based on the equation of the kinetic energy of a CME, we defined the potential CME eruption speed as follows:

$$V_{\text{CME}}^2 \text{ [km/s]} \approx c \left[ \frac{\text{km/s}}{G} \right] \frac{\iint B^2 / B_{\text{avg}} dA_1 \Delta}{\iint dA_2 \Delta}$$

$$2 \ln V_{\text{CME}} = \ln c + \ln \iint B^2 / B_{\text{avg}} dA_1 - \ln A_2$$

where  $c$  is a constant,  $B$  is the magnetic field in Gauss,  $A$  is an effective AR area, and  $\Delta$  is an effective AR volume. We are currently testing our analysis using the NSO/GONG magnetograms acquired during Solar Cycle 23 and 24.

## REFERENCES

- Jin, M., Manchester, W. B., van der Holst, B., et al. 2017, The Astrophysical Journal, 834, 173, doi: 10.3847/1538-4357/834/2/173
- Bradley, L., Sipőcz, B., Robitaille, T., et al. 2022, `astropy/photutils`: 1.5.0, 1.5.0, Zenodo, doi: 10.5281/zenodo.6825092
- Astropy Collaboration, Price-Whelan, A. M., Lim, P. L., et al. 2022, *ApJ*, 935, 167, doi: 10.3847/1538-4357/ac7c74
- Pedregosa, F., Varoquaux, G., Gramfort, A., et al. 2011, *Journal of Machine Learning Research*, 12, 2825
- Rousseau, P. J. 1987, *Computational and Applied Mathematics*, 20, 53, doi: 10.1016/0377-0427(87)90125-7
- Sharma, S. 1996, *Applied Multivariate Techniques* (New York: Wiley), 225, doi: 10.1002/9780470316757
- Mason, E. I., & Uritsky, V. M. 2022, *The Astrophysical Journal Letters*, 937, L19, doi: 10.3847/2041-8213/ac9124
- Steward, G., Lobzin, V., Cairns, I. H., Li, B., & Neudigg, D. 2017, *Space Weather*, 15, 1151, doi: 10.1002/2017SW001595

## ACKNOWLEDGEMENTS

This research is supported in part by NASA 80NSSC22K0268 and NSF ANSWERS 149771.

